THE USE OF DISCRETE ORDINATES METHOD FOR CALCULATION OF THE PHOTONEUTRON PRODUCTION IN TARGETS BOMBARDED BY ELECTRON BEAM

A. M. Voloschenko, Yu. V. Pomazan
Keldysh Institute of Applied Mathematics, Moscow, 125047, Miusskaya Sq., 4, Russia
volosch@kiam.ru

N. T. Kulagin
Institute of Physics and Power Engineering, Obninsk, 249020, Bondarenko Sq., 1, Russia
kulagin@ippe.obninsk.ru

ABSTRACT

The recommended files of photonuclear reactions of 164 isotopes are now available as a result of the IAEA coordinated research programme [1]. The possibility of the use of these evaluated data and the CEPXS-BFP/ROZ-6.5 package [2] for coupled electron-photon S_n calculations for calculation of the photo-neutron source in thick targets bombarded by electron beam is examined. A special utility that prepares the multigroup photoneutron production matrix for mixtures, based on the use of the photonuclear data for nuclides stored in the ACE format, has been developed. The energy range of incident electrons in our investigation is from the photonuclear threshold up to 150 MeV. Our results are compared with the experimental data when available and Monte Carlo calculations with a recent version of the MCNPX code [3], based on the use of the same recommended files of photonuclear reactions [1]. We show that the agreement between S_n calculations and both experimental and Monte Carlo results is satisfactory if the energy mesh, used in the CEPXS-BFP/ROZ-6.5 calculations, is sufficiently fine to describe the photoneutron production in the vicinity of the Giant Dipole Resonance (GDR). The possibility of calculation of photoneutron production can be used both for estimation of radiation fields in the vicinity of high-energy electron accelerators and in the study of electron beam based ADS systems [4].

1. INTRODUCTION

The use of the S_n method for coupled neutral-charged particle calculations gives an essential computational gain in comparison with the Monte Carlo method both in solving deep-penetration transport problems and if the detailed information about energy, spatial and (or) angular distributions of particle fluxes is required. To perform calculations of the electron beam generated photoneutron production by the S_n method the coupled electron-photon-hadron multigroup cross-sections are required. Now the CEPXS-BFP [2] code that is the adapted version of the multigroup coupled electron-photon cross-sections generating code CEPXS [5] is available, where the following new options, based on the "Monte Carlo" option of CEPXS [6], are available: "*the Sn-CSD"* option, where the continuous slowing down (CSD) operator is treated directly, but the continuous-scattering operator is treated indirectly in the P_L approximation, and "*the Sn-BFP"* option, where both the CSD and continuous-scattering operators of the Boltzmann-Fokker-Planck (BFP) equation are treated directly. The CEPXS-BFP code can generate coupled electron-photon cross-sections for energy range

from 1 KeV up to 1 GeV that can be, due the new cross-sections interface [2], efficiently used by the S_n code ROZ-6.5, where the possibility of the direct treatment both the CSD and continuous-scattering operators has been implemented.

The IAEA recommended files of photonuclear reactions of 164 nuclides are now available [1]. Starting from version 67 the NJOY99 code [7, 8] can generate with the use of these data the fully-coupled neutron-photon multigroup cross-sections where the photoneutron production is included. (Unfortunately, not all files from library [1] satisfy to a formal requirement to be processed by the NJOY99.67 code). Before this possibility has been implemented in NJOY99, we have developed the PHOTON_ACE utility that can prepare the multigroup photoneutron production matrix for mixtures. This utility is based on the use of the photonuclear class 'u' ACE format, defined in [3]. This format is specially developed to store the photonuclear data for nuclides and can be generated, for example, by NJOY99 code. Typically, this format is used by the current versions of MCNP4C2 and MCNPX codes [3].

Of course, the possibilities of the PHOTON_ACE utility are very limited in comparison with the NJOY99.67 code. But, as will be demonstrated, it can be used for estimation of the photoneutron production until the coupled electron-photon-neutron multigroup cross-sections libraries will be available.

Next, the CEPXS-BFP/ROZ-6.5 package for coupled electron-photon calculations with treatment of the charged particles transport on the base of the BFP equation has been enhanced with the capability for calculation of the photo-neutron source with the use of the photoneutron production matrix, generated by the PHOTON_ACE utility. This possibility is desirable for estimation of radiation fields in the vicinity of high-energy electron accelerators and can be also used in the study of electron beam based ADS systems. Both experimental and calculation results show that the neutron yield from the lead target bombarded by 100 MeV electron beam is essentially (about three orders) less than bombarded by 1 GeV proton beam. But due more stable and intense currents, available now for electron accelerators, the electron beam based ADS systems may have some advantages in comparison with the high-energy proton beam based ones.

The organization of the paper is as follows. In Sec. 2 the algorithm used for calculation of the photo-neutron source is described. In Sec. 3 the calculated total neutron yields for copper and lead targets of different thickness are given in comparison with experimental and Monte Carlo data. The results of calculation of differential photo-neutron source spectra for energies of the electron beam 140 and 150 MeV for copper and lead targets, respectively, are also presented in this section. Finally, conclusions are given.

2. THE ALGORITHM FOR CALCULATION OF THE PHOTO-NEUTRON SOURCE

Information about photoneutron production cross-sections for a nuclide both in the ENDF and ACE formats is given in the following form

$$\sigma(\mu, E, E') = \sigma(E) y(E) f(\mu, E, E') \big/ 2\pi \,, \qquad (1)$$

where E is the incident photon energy, E' is the energy of the neutron emitted with cosine $\mu = Cos\theta = (\vec{\Omega}, \vec{\Omega}')$, $\sigma(E)$ is the interaction cross-section, $y(E)$ is the neutron yield or multiplicity, and $f(\mu, E, E')$ is the normalized photo-neutrons distribution, represented by using the Kalbach-Chadwick distribution

$$f(\mu,E,E') = f_0(E,E')\left[\frac{a(E,E')}{\sinh(a(E,E'))}\left[\cosh(a(E,E')\mu) + r(E,E')\sinh(a(E,E')\mu)\right]\right], \qquad (2)$$

$$\int dE' \int d\mu f(\mu,E,E') = 1, \qquad \int dE' f_0(E,E') = 1. \qquad (3)$$

In Eq. (2) $f_0(E,E')$ is the probability density function, $a(E,E')$ is the angular distribution slope value, and $r(E,E')$ is the pre-compound fraction, $0 \le r \le 1$. In ACE format information about functions $\sigma y(E)$, $a(E,E')$, $r(E,E')$ and $f_0(E,E')$ is available for some sufficiently fine incident photon energy grid $\{E_k\}$, and for a set of neutron emission energy grids $\{E'_{j,k}\}$; distributions $a(E,E')$ and $f_0(E,E')$ are given in the form of histograms in variable E'. Typical form of photoneutron production cross-section $\sigma y(E)$ is given in Figure 1.

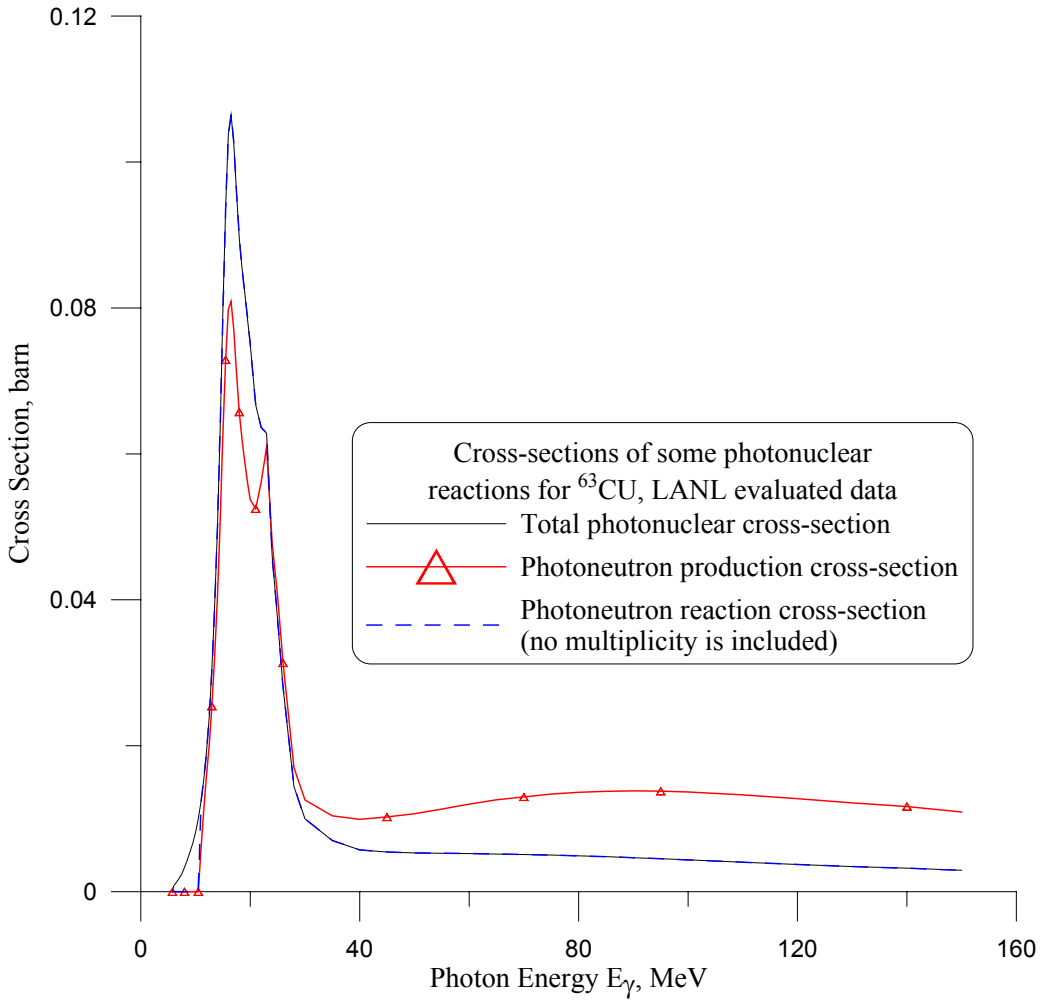

Figure 1. Cross-sections of some photonuclear reactions for ^{63}Cu, taken from LANL evaluated data.

This information is sufficient to calculate the P_L harmonics of the macroscopic cross-section $\Sigma_{s,l}^{p(\gamma)\to q(n)}$ of production of a neutron in group $q(n)$ by a photon from group $p(\gamma)$, needed to calculate the photo-neutron source. For plane geometry case this source is

$$S^{q(n)}(x,\mu)=\sum_{l=0}^{L}\frac{2l+1}{4\pi}\sum_{p(\gamma)=1}^{P(\gamma)}\Sigma_{s,l}^{p(\gamma)\to q(n)}P_l(\mu)\phi_l^{p(\gamma)}(x)\,, \tag{4}$$

where $\phi_l^{p(\gamma)}(x)$ is the l-th angular moment of the photon angular flux $\psi^{p(\gamma)}(x,\mu)$ for group $p(\gamma)$,

$$\phi_l^{p(\gamma)}(x)=2\pi\int_{-1}^{1}P_l(\mu)\psi^{p(\gamma)}(x,\mu)d\mu\,, \tag{5}$$

$P(\gamma)$ is the total number of photon groups. For calculation of the scalar photo-neutron source $S^{q(n)}(x)$ only the zeroth harmonic of the neutron production cross-section is required:

$$S^{q(n)}(x)=\sum_{p(\gamma)=1}^{P(\gamma)}\Sigma_{s,0}^{p(\gamma)\to q(n)}\Phi^{p(\gamma)}(x)\,, \tag{6}$$

where $\Phi^{p(\gamma)}(x)\equiv\phi_0^{p(\gamma)}(x)$ is the scalar photon flux. In calculation of $\Sigma_{s,0}^{p(\gamma)\to q(n)}$ parameters $a(E,E')$ and $r(E,E')$ of the Kalbach-Chadwick distribution (2) are not used. If the energy mesh for photons is sufficiently fine the following simple formula can be used to calculate $\Sigma_{s,0}^{p(\gamma)\to q(n)}$

$$\Sigma_{s,0}^{p(\gamma)\to q(n)}=\sum_i\rho_i(\sigma y)_i^{p(\gamma)}f_{0,i}^{p(\gamma)\to q(n)}\,, \tag{7}$$

where ρ_i is the nuclear density of the i-th nuclide in a mixture,

$$(\sigma y)_i^{p(\gamma)}\approx\sigma y_i(\tilde{E}^{p(\gamma)})\,,\qquad f_{0,i}^{p(\gamma)\to q(n)}\approx\Delta E_{q(n)}\tilde{f}_{0,i}(\tilde{E}^{p(\gamma)},E^{q(n)})\,, \tag{8}$$

where $\tilde{E}^{p(\gamma)}$ is a midpoint of the photon group $p(\gamma)$ energy interval, and the probability density function $\tilde{f}_{0,i}(E,E')$ is received by recalculation of a histogram in the second variable from original emission energy grid to output emission energy grid. In the utility PHOTON_ACE the output emission energy grid can be received both as result of joining up of emission grids for all incident energies and nuclides used, and can be defined by a user.

3. NEUTRON YIELDS FROM TARGETS BOMBARDED BY ELECTRON BEAM

In this section we present results of CEPXS-BFP/ROZ-6.5 S_n calculations of the total neutron yields for plane copper and lead targets, bombarded by the perpendicularly incident electron beam, in dependence on the electron beam energy and target thickness and in comparison with experimental data, when available, and Monte Carlo calculations, performed with the use of the MCNPX code [3].

In our calculations the natural isotopic abundance's were used both for the copper (^{63}Cu (69.17%) and ^{65}Cu (30.83%)) and lead (^{204}Pb (1.4%), ^{206}Pb (24.1%), ^{207}Pb (22.1%) and ^{208}Pb (52.4%)) targets. The LANL and KAERI photonuclear data files [1] were used for ^{63}Cu ^{206}Pb, ^{207}Pb, ^{208}Pb and ^{65}Cu isotopes, respectively. Due the absence of photonuclear data for ^{204}Pb isotope in library [1], we have increased the abundance of ^{206}Pb to 25.5% (in assumption that properties of ^{204}Pb and ^{206}Pb isotopes are similar) in calculations of the lead photoneutron production matrices.

Due the one-dimensional nature of ROZ-6.5 code, it was also supposed that the incident electron beam is sufficiently wide. Received in this approximation results give the upper bound of the possible neutron yields from a target with a given thickness and material. So, the results obtained with the use of CEPXS-BFP/ROZ-6.5 package in the assumption that the used electron-photon-neutron cascade

model is sufficiently accurate should slightly overestimate the pencil beam (with the spot of 1.27 cm in diameter [10]) experimental results.

Next and most important limitation is the completeness of the electron-photon-hadron cascade model used. Unfortunately, it is not fully coupled and no hadron cascade transport is included. This is a limitation of the multigroup cross-sections available but not a limitation of the ROZ-6.5 code that is a 1D S_n multiparticle neutral-charged cascade transport problem solver.

The energy grids, spatial and angular meshes, and the order of scattering anisotropy were chosen sufficiently fine to make an approximation error small in comparison with the error that is defined by an approximate nature both the cross-sections and the electron-photon-neutron cascade model used. The "*full coupling*" and "*Sn-CSD"* options of the CEPXS-BFP code were used to generate the multigroup electron-photon cascade cross-section sets. Numerical experiment has shown that the use of the "*Sn-BFP"* option of the code gives the similar results. The typical used approximations are given in Table 1. The same energy grids were used both for electrons and photons. The cutoff energy in electron-photon cascade calculations was chosen 9.0 and 5.5 MeV for copper and lead targets, respectively, to be below the photoneutron production thresholds: 9.91 and 6.74 MeV for copper and lead, respectively. The neutron emission energy grid was chosen from photonuclear data files.

Table 1. Approximations used for calculation of the photo-neutron source.

Energy of incident electrons (MeV)	Number of electron/photon groups	Type of energy grid used	Order of S_n and P_L approximations	Number of neutron groups
<25.0	40	linear	$S_{32}P_{31}$	15-78
<50.0	50	linear	$S_{32}P_{31}$	82-131
50.0	50	logarithmical	$S_{32}P_{31}$	163-191
100.0	60	logarithmical	$S_{64}P_{63}$	240-266
140.0, 150.0	70	logarithmical	$S_{64}P_{63}$	275-304

Results of calculations of the total neutron yields for copper and lead targets are presented in Tables 2-5 and 6-9, respectively. In these tables X_0 is the radiation length. For copper $X_0 = 12.86\, g/cm^2 \approx 1.4353\ cm$ and for lead $X_0 = 6.37\, g/cm^2 \approx 0.5612\ cm$.

Table 2. Experimental and calculated neutron yields for 1.48 cm $\approx 1X_0$ thick copper target.

Energy (MeV)	Reported Yield [10] (10^{-3} n/e)	MCNPX Yield [3] (10^{-3} n/e)	Ratio MCNPX/ Experimental	CEPXS-BFP/ ROZ6.5 Yield (10^{-3} n/e)	Ratio CEPXS-BFP/ROZ6.5/ Experimental
16.1	0.03 ± 0.0045	0.0321	1.07	0.0374	1.25
21.2	0.26 ± 0.039	0.218	0.84	0.251	0.97
28.3	0.82 ± 0.123	0.627	0.76	0.721	0.89
34.3	1.29 ± 0.19	0.963	0.75	1.10	0.85
35.5	1.39 ± 0.21	1.02	0.73	1.16	0.83
100.0				2.95	
140.0				3.48	

Table 3. Experimental and calculated neutron yields for 2.96 cm $\approx 2X_0$ thick copper target.

Energy (MeV)	Reported Yield [10] (10^{-3} n/e)	MCNPX Yield [3] (10^{-3} n/e)	Ratio MCNPX/ Experimental	CEPXS-BFP/ ROZ6.5 Yield (10^{-3} n/e)	Ratio CEPXS-BFP/ROZ6.5/ Experimental
16.1	0.05 ± 0.0075	0.0538	1.08	0.0625	1.25
21.2	0.43 ± 0.065	0.374	0.87	0.434	1.01
28.3	1.39 ± 0.21	1.12	0.81	1.31	0.94
34.3	2.37 ± 0.36	1.80	0.76	2.09	0.88
100.0				7.81	
140.0				9.90	

Table 4. Experimental and calculated neutron yields for 4.45 cm $\approx 3X_0$ thick copper target.

Energy (MeV)	Reported Yield [10] (10^{-3} n/e)	MCNPX Yield [3] (10^{-3} n/e)	Ratio MCNPX/ Experimental	CEPXS-BFP/ ROZ6.5 Yield (10^{-3} n/e)	Ratio CEPXS-BFP/ROZ6.5/ Experimental
16.1	0.07 ± 0.0105	0.0676	0.97	0.0778	1.11
21.2	0.53 ± 0.080	0.471	0.89	0.547	1.03
28.3	1.80 ± 0.27	1.43	0.79	1.68	0.93
34.3	2.93 ± 0.44	2.33	0.79	2.71	0.92
100.0				11.5	
140.0				15.5	

Table 5. Experimental and calculated neutron yields for a "semi-infinite" (28.7 cm $\approx 20X_0$ thick) copper target.

Energy (MeV)	Reported Yield [11] (10^{-3} n/e)	MCNPX Yield [3] (10^{-3} n/e)	Ratio MCNPX/ Experimental	CEPXS-BFP/ ROZ6.5 Yield (10^{-3} n/e)	Ratio CEPXS-BFP/ROZ6.5/ Experimental
15.0	0.0481 ± 0.0096	0.0457	0.95	0.0543	1.13
20.0	0.5 ± 0.100	0.472	0.94	0.556	1.11
25.0	1.42 ± 0.28	1.31	0.92	1.56	1.10
34.0	3.46 ± 0.69	3.19	0.92	3.76	1.09
50.0	7.02 ± 1.4	6.44	0.92	7.68	1.09
100.0	17.5 ± 0.35	15.9	0.91	18.8	1.07
140.0				27.8	

Table 6. Experimental and calculated neutron yields for 0.518 cm $\approx 1X_0$ thick lead target.

Energy (MeV)	Reported Yield [10] (10^{-3} n/e)	MCNPX Yield [3] (10^{-3} n/e)	Ratio MCNPX/ Experimental	CEPXS-BFP/ ROZ6.5 Yield (10^{-3} n/e)	Ratio CEPXS-BFP/ROZ6.5/ Experimental
18.7	0.73 ± 0.11	0.563	0.77	0.513	0.70
28.3	1.69 ± 0.25	1.33	0.79	1.23	0.73
34.5	2.12 ± 0.32	1.60	0.75	1.48	0.70

100.0		3.16 [9]		2.50	
150.0		4.01 [9]		2.86	

Table 7. Experimental and calculated neutron yields for 1.52 cm $\approx 3X_0$ thick lead target.

Energy (MeV)	Reported Yield [10] (10^{-3} n/e)	MCNPX Yield [3] (10^{-3} n/e)	Ratio MCNPX/ Experimental	CEPXS-BFP/ ROZ6.5 Yield (10^{-3} n/e)	Ratio CEPXS-BFP/ROZ6.5/ Experimental
18.7	1.77 ± 0.27	1.35	0.76	1.23	0.69
28.3	4.69 ± 0.70	3.81	0.81	3.50	0.75
34.5	6.46 ± 0.97	5.15	0.80	4.77	0.74
100.0				13.2	
150.0				17.1	

Table 8. Experimental and calculated neutron yields for 3.03 cm $\approx 6X_0$ thick lead target.

Energy (MeV)	Reported Yield [10] (10^{-3} n/e)	MCNPX Yield [3] (10^{-3} n/e)	Ratio MCNPX/ Experimental	CEPXS-BFP/ ROZ6.5 Yield (10^{-3} n/e)	Ratio CEPXS-BFP/ROZ6.5/ Experimental
18.7	2.50 ± 0.38	1.84	0.74	1.69	0.68
28.3	6.67 ± 1.00	5.37	0.80	4.91	0.74
34.5	9.00 ± 1.35	7.41	0.82	6.85	0.76
100.0		31.6 [9]		23.5	
150.0		40.1 [9]		34.4	

Table 9. Experimental and calculated neutron yields for a "semi-infinite" (11.22 cm $\approx 20X_0$ thick) lead target.

Energy (MeV)	Reported Yield [11] (10^{-3} n/e)	MCNPX Yield [3] (10^{-3} n/e)	Ratio MCNPX/ Experimental	CEPXS-BFP/ ROZ6.5 Yield (10^{-3} n/e)	Ratio CEPXS-BFP/ROZ6.5/ Experimental
10.0	0.0322 ± 0.0064	0.0283	0.88	0.0163	0.51
15.0	0.983 ± 0.197	0.750	0.76	0.640	0.65
20.0	3.27 ± 0.65	2.72	0.83	2.47	0.76
25.0	5.73 ± 1.15	4.88	0.85	4.49	0.78
34.0	9.64 ± 1.93	8.56	0.89	7.98	0.83
50.0	15.8 ± 3.2	14.5	0.92	13.9	0.88
100.0	33.6 ± 6.7	31.5	0.94	31.2	0.93
150.0				48.7	

We should note that both experimental and Monte Carlo yields for the "semi-infinite" targets (Tables 5 and 9) do not include the neutron transport and absorption within the material [3]. So, only the neutron production is given. Similar model is used also in CEPXS-BFP/ROZ6.5 calculations.

In general, the comparative agreement between our calculations and both experimental data and Monte Carlo calculations for copper targets is rather good. The maximum available electron beam

energy 140 MeV for copper targets in Tables 2-5 is defined by the upper energy bound of available in KAERI photonuclear data file cross-sections for ^{65}Cu .

For the lead targets calculated by CEPXS-BFP/ROZ6.5 package yields are slightly (but systematically) less than experimental data. Probably, the main reason of this underestimation is the absence of the hadron transport in our calculations. The primary photo-neutrons can generate secondary neutrons. Maybe, the photo-protons and secondary protons, which also can generate neutrons, should be also included. We note also that, in general, the accuracy of predictions is less in the vicinity of the photonuclear threshold.

Next, we present (see Figures 2 and 3) some calculated spectral distributions of the photo-neutron source, averaged in a target volume. It is difficult to validate these results as no experimental data are known for both angular and energy distributions of photo-neutrons.

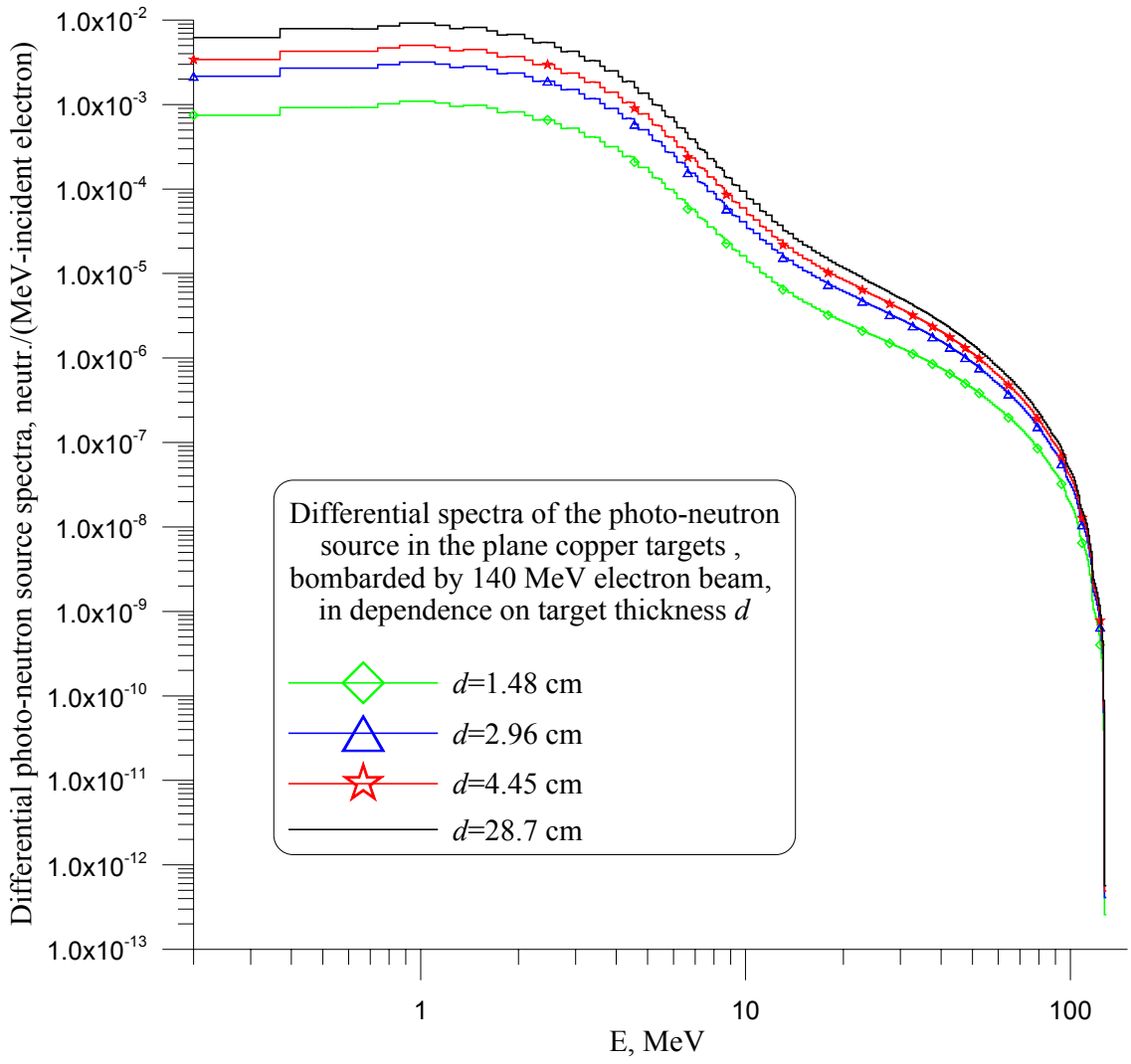

Figure 2. Differential photo-neutron source spectra in the plane copper targets, bombarded by 140 MeV electron beam that is perpendicularly incident on the target, in dependence on the target thickness d, calculated in $S_{64}P_{63}$ approximation. The spectra are averaged over the target thickness and normalized per 1 incident electron.

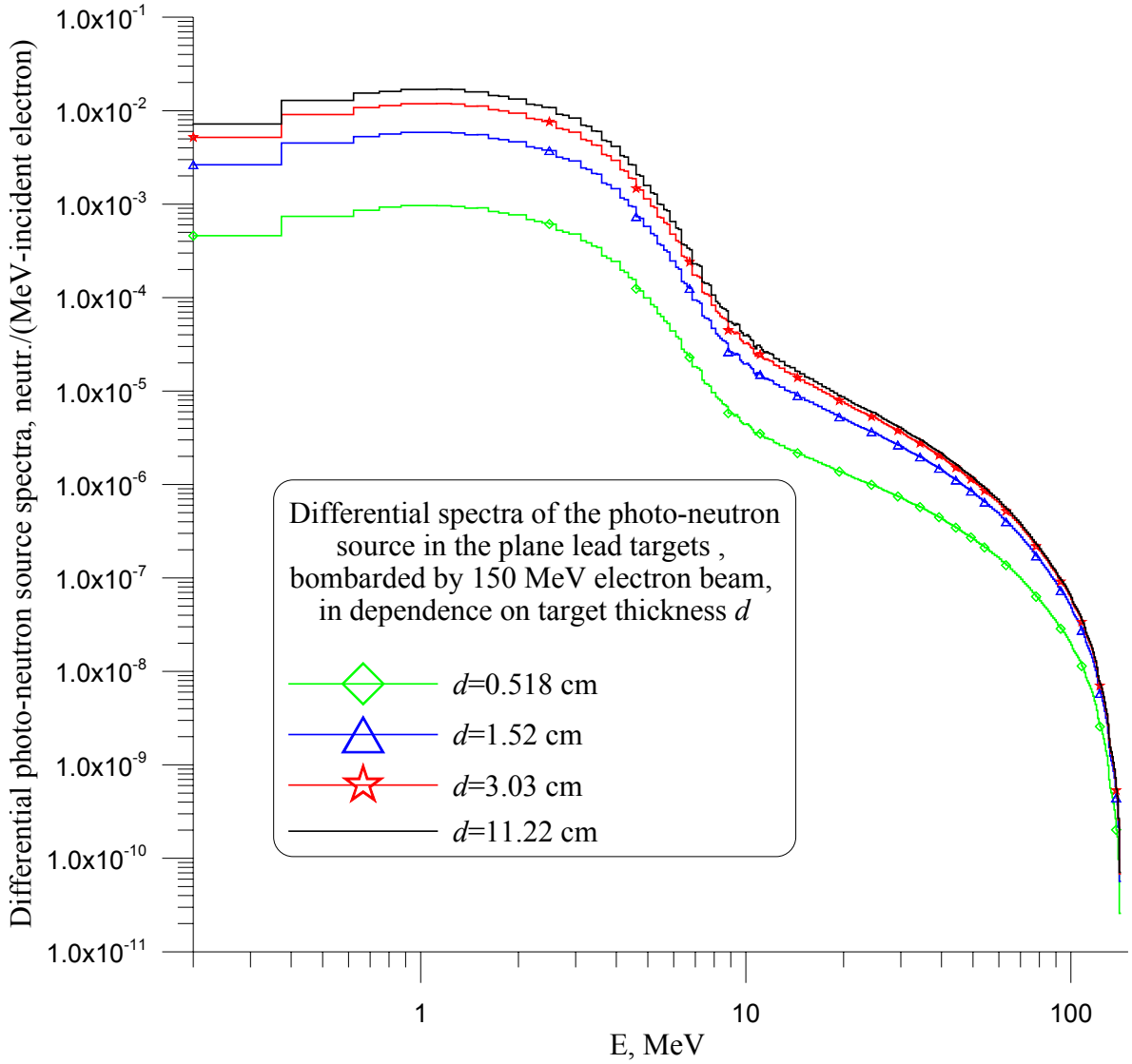

Figure 3. Differential photo-neutron source spectra in the plane lead targets, bombarded by 150 MeV electron beam that is perpendicularly incident on the target, in dependence on the target thickness d. The $S_{64}P_{63}$ approximation is used. The spectra are averaged over the target thickness and normalized per 1 incident electron.

CONCLUSIONS

The use of the S_n method for coupled neutral-charged particle calculations gives an additional computational tool for solving electron-photon-hadron cascade problems. Due the new cross-section interface [2] multiparticle cascade 1D problems can be efficiently solved by ROZ-6.5 code. The main computational difficulties in the use of S_n codes for solving electron-photon-hadron cascade problems, especially in 2D and 3D geometries, are defined by the highly-anisotropical nature of electron (and photon) scattering. This requires both the use of a specially constructed schemes for acceleration of inner iterations convergence and improvements in approximation of scattering anisotropy.

Numerical results show that to receive an acceptable accuracy in prediction of photo-neutron yields for a wide range of nuclides the fully coupled model of electron-photon-hadron cascade should be used. Potential possibility to prepare multigroup cross-sections for this model is just opened by the last updates in the NJOY99 code [8] and the current progress in construction of evaluated data in ENDF format both for photonuclear [1] and high-energy hadron cross-sections.

Additional experimental data are needed to benchmark both available photonuclear evaluations and electron-photon-hadron cascade calculations. These data should include measurements of total, angular and energy distributions of photo-neutron yields for sufficiently wide range both target materials and energy of the incident electron beam.

ACKNOWLEDGEMENTS

This work was performed, in part, under auspices of the International Science and Technology Center, grant No. 1486.

REFERENCES

1. Handbook on photonuclear data for applications, IAEA TECDOC Draft No. 3, March 2000.
2. A. M. Voloschenko, "An Experience in the Use of the Sn Method for Hadron and Electron-Photon Transport Problems in Boltzmann-Fokker-Planck Formulation," *Proc. of short course Neutron and Radiation Transport Simulation: Theory and Applications*, edited by Prof. Nam Zin Cho, KAIST, Taejon, Korea, February 19-22, 2001, p. 319.
3. M. C. White, "Development and Implementation of Photonuclear Cross-Section Data for Mutually Coupled Neutron-Photon Transport Calculations in the Monte Carlo N-Particle (MCNP) Radiation Transport Code," Thesis, LANL, LA-13744-T, July 2000.
4. P. Vertes, D. Ridikas, "Some test calculation with the IAEA Photonuclear Data Library," to be published in *"Proc. of Intern. Conf. on Nuclear Data for Science and Technology,"* Tsukuba, Japan, Oct. 7-12, 2001.
5. L. J. Lorence, Jr., J. E. Morel and G. D. Valdez, "Physics Guide to CEPXS: A Multigroup Coupled Electron-Photon Cross-Section Generating Code," Version 1.0, SAND89-1685, Sandia National Laboratories (1989).
6. J. E. Morel, L. J. Lorence, Jr., R. P. Kensek, J. A. Halbeib, D. P. Sloan, "A Hybrid Multigroup/Continuous-Energy Monte Carlo Method for Solving the Boltzmann-Fokker-Planck Equation," *Nucl. Sci. Eng.,* **124**, 369 (1996).
7. R. E. MacFarlane, "Readme0," LANL, December 31, 1999; NJOY99 Code System for Producing Pointwise and Multigroup Neutron and Photon Cross-Sections from ENDF/B Data, RSICC Code Package PSR-480.
8. R. E. MacFarlane, "Readme67," LANL, February 12, 2002.
9. P. Vertes, "Test calculation with the IAEA Photonuclear Data Library," INDC(HUN)-035, 2001.
10. W. C. Barber, W. D. George, "Neutron Yields from Targets Bombarded by Electrons," *Phys. Rev.*, **116**, 1551 (1959).
11. W. P. Swanson, "Improved Calculation of Photo-Neutron Yields Released By Incident Electrons," *Health Physics*, **37**, 347 (1979).